Analysis of Metal Deformation in Pilgering of Nuclear Reactor

Critical Analysis on Metal Deformation of Pilgering in NR

MD.Sirajuddin, Balabhadruni Sai Kumar, B.Sharan Kumar, Koppaka Jahanavi, Sriram Shilpa, Asuri Harika,
Dept. of Electronics and Communication Engineering,
Chilkur Balaji Institute of Technology (CBTV),
Affiliated To JNTU,
Hyderabad, India,
Email: saikumarbalabhadruni@gmail.com.

Abstract— In the field of Tooling and process of Piercing, Extrusion, Cold Pilgermills and their forces analysis. We have studied and analyzed operations carried out in various equipment's in EPP and BPS. The 37801 Extrusion press and Piercing 1200T at piercing of NFC is used for extrusion of various materials. Extrusion is defined as the process of shaping the material by forcing in to flow through a shaped opening from a die. It is used to create objects of fixed cross sectional profiles; the material is pushed through the die of the desired cross section. The Expansion and Extrusion process is studied using both EPP and BPS and losses are calculated. Pilgering is a tube reduction process, where the outer diameter and the thickness of a tube are simultaneously reduced between the reciprocating grooved dies and a fixed mandrel, exclusive NFC this process is uses all over the world for the manufacturing of fuel clad tubes and structural requirements for nuclear reactors. The diameter and the wall thickness of the ingoing tube are reduces by applying large amount of forces causing high amount of plastic deformation, increasing length and ultimate strength of the tube, distribution of stress and resultant forces on the tube plays a vital role in cold working process resulting in plastic deformation of the metal, analysis of metal deformation of seamless tube during pilgering process is very complex. So a simplified analysis is proposed in the work to understand the metal deformation of the seamless tube in Pilgering.

Keywords—Pilgering; Extrusion; Mandrel; Expansion; deformation; clad-tubes; nuclear reactors; stress; Tooling.

I. INTRODUCTION

Pilgering is a consistent tube structuring operation where the inward span and divider thickness are both continuously lessened between a settled pivot symmetric mandrel and forward and retrogressive moving notched bites the dust. The name – Pilgering is gotten from the German word "pilger" which intends to-and-fro movement. In pilgering pass on moves over the tube here and there and then here again and subsequently the name pilgering is picked for the procedure.

The mandrel and die groove areas relate through a rack and pinion framework, giving generally a rolling-without-sliding development pressing the tube between the pass on furrows and the mandrel. Pilgering is by and large picked for its dimensional exactness and great composition advancement, controlled by the proportion of thickness to breadth lessening.

The procedure is semi occasional, comprising of a few many strokes between which the tube is turned and advanced (by a little separation, the advances by a couple of mm down the 300mm long disfigurement zone of the mandrel. It takes 80-100 strokes before the disfigurement is finished. Besides, because of pivot, the molecule is moved at every new stroke in the distinctive parts of the depression, in this way under diverse strain and anxiety conditions. Therefore the metal experiences a progression of little incremental plastic strains On the other hand under elastic and compressive hassles. This complex history now and again brings about imperfections, for example, transverse breaks or surface harms by low-cycle moving contact exhaustion, probably at areas where micro structural heterogeneities concentrate harm.

The principle distinction in the middle of drawing and pilgering is that drawing is performed under strain while pilgering is pressure framing procedure. The frosty drawing procedure has an innate issue of rapidly getting depleted of material pliability due to connected with malleable anxieties. However in pilgering, better cross-sectional diminishments are allowed which completely use the material's pliancy saves. Besides, numerous materials have 35-40% more formability under compressive strengths. All these gimmicks support the utilization of pilgering methodology for tube creation. Additionally, chilly pilgering can be utilized to move numerous sorts of high quality materials, which are extremely hard to be lessened by drawing.

The tube extension in pilgering methodology is accomplished by lessening of the external and internal breadth, and additionally the divider thickness of the ingoing tubes. The frosty pilgered tube is portrayed by little dimensional varieties and a high hardness levels and hence an excellent and fantastic mach inability.

II. BACKGROUND AND DESCRIPTION

A. Description Of Schematics

Toward the start of the stroke or the pass the round area framed between the notches of the two restricting moves compares to the measurement of the ingoing tube and to the thickest segment of the mandrel. As the moves get up and go over the round area lessens in zone until, toward the end of

the pass length the roundabout segment compare to the completed inward measurement of the tube.

The inward surface of the tube is balanced by a level axi symmetric mandrel, held by mandrel pole. The assessment of the breadth of the mandrel along the moving course is one of the parameter controlling the last tube quality. Two passes on with non axi-symmetric depressions, placed in a here and there and then here again moving "seat", shape the outer development giving generally a moving without sliding development pressing the tube between the kick the bucket groove and the mandrel.

The conjugation of the mandrel profile and the pass on depression profile controls the assessment of the measurement and the tube. After each over and over again development of the passes on, a little length of the tube performs bolster forward carriage, and pivoted by a settled point.

There is small gap between the two dies and henceforth back and forth movement of the die on certain measure of ovality is instigated in the shaped tube shape. To diminish the ovality the tube is turned by a point each pass of the same parcel of the tube does not generally fall in the bite the dust holes and ovality is shaped at diverse plot of the tubes in the distinctive passes. As the same share of the tube experiences such a variety of passes of the distortion before it leaves the plant the ovality at first is steadily lessened lastly when the tube leaves the pilger process almost no measure of the ovality is discovered to be there in the tube. The edge is picked such that after every pass a certain point on the surface of the tube does not possess the same piece of the factory.

B. Advantages of cold pilgering

- It is evident from the above that cold pilgering is efficient in producing larger reductions in less number of passes and thus quantity of production. The pilgered tubes are characterized by higher tensile and yield strength, superior surface conditioning, high diameter to wall thickness ratios, higher dimensional tolerances and enhanced mach-inability.
- Cold pilgering provides with improved properties and dimensional tolerances compared to hot finished tubing process. The cross-section reductions attained are higher than those achieved by other processes. Because the cold pilgering process applies pressure from all sides, it can achieve reductions up to 90 percent for copper; 80 percent for stainless steel, nickel alloys, and Zircaloy and 75 percent for high-strength titanium alloys. Cold pilgered tubes also offer enhanced mach-inability and wall thickness of outside diameter.
- The tube manufacturers use cold pilgering to modify sizes, properties and surface finish to the advantages of the customers. Cold pilgering results in less stock removal, saving cost of boring and loss of chips. Pilgering significantly lengthens the base material and internal diameter.
- By taking the advantage of the ability of the cold pilgering to increase the length of the base material as it reduces the wall thickness, expensive bore operation can often be performed on short length base material, rather than the longer length final tube product. This often generates significant savings on customers.

C. Current Scenario of Fuel Tubes

Presently, the tubes being used to manufacture nuclear fuel bundles are mainly Zircalloy tubes. They fulfil the requirements of PHWRs (Pressurized Heavy Water Reactors). They use Natural (non- enriched) Uranium as a fuel. Since the fuel is non-enriched, the useful portion of the fuel (U-235) is around 0.7% only. Thus, it becomes critical to check the absorption of neutrons as they are produced in relatively less quantities. This is the main reason for using Zircalloy as its "neutron absorption characteristics" are very low. Also, they use Deuterium Oxide (D2O) as moderator. D2O, as compared to water (H2O) also has very less neutron absorption tendency. Thus they offer minimum resistance to the passage of neutrons through them which is a very critical property to sustain chain reaction.

Another type of reactors, which are in use in India are BWRs (Boiling Water Reactors). They use enriched Uranium as fuel. Thus, the useful portion of the fuel (U-235) is much more than 0.7% and hence, there is an abundance of neutrons. They use a different grade of zirc alloy as fuel tube material but they use normal water (H2O) as moderator. Here, though the neutron absorption characteristics of H2 O are very high, we can overlook them as the neutrons are available in abundance.

II. ANALYZING METAL WORKING PROCESSES

The prerequisite of a hypothesis or theories for portraying the mechanics of a metal working procedure is the capacity to make a precise forecast of the Strain, Stress and speeds at every point in the disfigured district of the subject or work piece. Methodologies contrast in unpredictability and in the extent to which they meet this prerequisite. Such speculations comprise of three sets of comparisons:

1. Relationship between Stress & Strain
2. Yield Criterion
3. Static equilibrium of force equations.

Conventionally there are nine unconstrained equations containing 9 unknowns, 6 stress and 3 strain components. While a systematic arrangement is conceivable if a sufficient number of limit conditions are defined, the scientific challenges and mathematical debugging in a general arrangement are quite formidable aspects. Consequently, most analyses of actual metal working methods are constrained to 2D or symmetric 3D issues

Analysis Methodologies:

- Finite element method, where a technique called matrix method with considerable reduction in computational time allowing huge increments of deformation for rigid plastic material.
- Slip line field theories permit p2p calculations of stress for plane strain conditions
- Lower & Upper Bound solutions which bases on the theory of limit analysis, using reasonable stress and velocity fields to calculate the boundaries where actual forming lies.

- The slab method assumes homogeneous deformation.
- Calculating average forming stress from the work of plastic deformation using Uniform deformation energy method.

III. AVENUE OF APPROACH

A. Analytical Model of Cold Pilgering Process:

Since pilgering is a very complex mechanical process, it is a herculean task to develop a model that exactly simulates the mechanical conditions during the process. So a simplified analysis was developed to make a technical model to study pilgering process. To start with, a feed element of length f is considered, and all the parameters of this element as it travels through the entire working length are studied. The length of feed element changes to Δxi due to partial elongation at every ith shot and is also turned by 60° and the position of the feed element changes as it travels through the working zone length as shown in the figure.

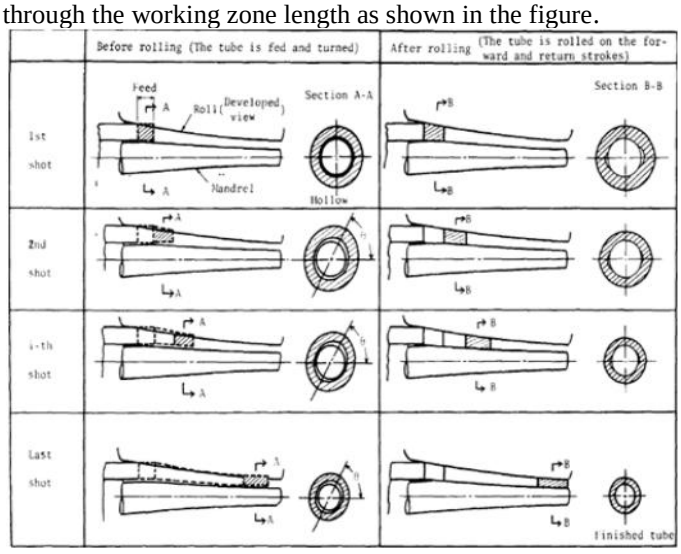

Fig [1]: Tube Before rolling and After rolling

According to volume-constancy condition, Δx_i is given by:

$$\Delta x_i = f * \frac{A_o}{A_i}$$

Where,

$\boldsymbol{A_o}$ =cross-sectional area of a hollow

$\boldsymbol{A_i}$ = cross-sectional area of a deformed tube element at the i^{th} shot.

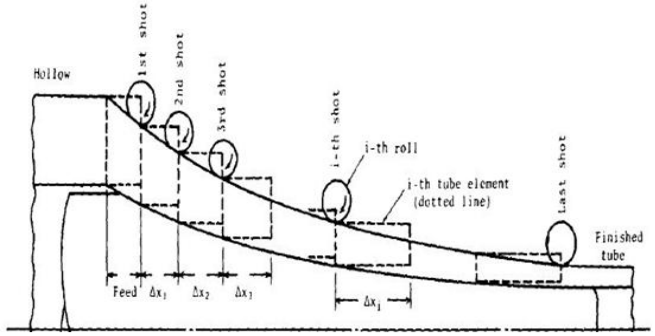

Fig [2]: tube cross section showing hollow to finished tube.

B. Partition of Tube Section:

The tube section under deformation is divided into two parts, i.e., the groove part and the flange part. The inside surface of the former is in contact with the mandrel, while the flange part is only in contact with the roll.

The material of the groove is deformed under outside pressure, inside pressure, circumferential compression and axial compression, while on the other hand the material of the flange part is deformed under low outside pressure, circumferential compression and axial tension.

The tube section is divided into three sections as shown in the figure. Section 1 & 2 belong to the groove part and the section 3 is the flange part. For simplicity, the deformation of each of the sections is assumed to be axi-symmetrical

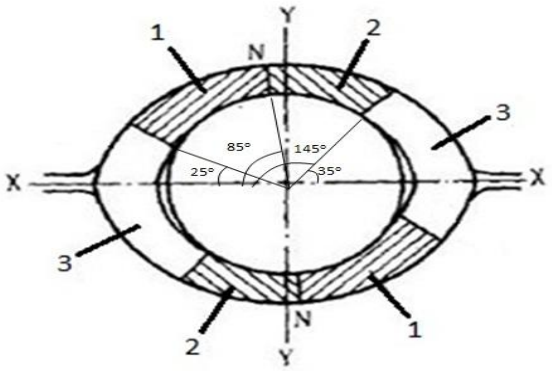

Fig [3]: The deformation of tube in cross-section.

C. Derivation Of Groove And Mandrel Profile Equations

1) Derivation Of Groove Profile Equation:

$$\boldsymbol{D_x = D_f + C_x(D_l - D_f - Z - L_i) + \frac{x}{L} * Z + n_x(L_i + L_a)}$$

Where ,

D_x= Groove diameter at point 'x' of the working section of the groove.

C_x= Factor for the shape of the groove and mandrel curve.

D_l = Outside diameter of the ingoing tube.

D_f= Outside diameter of the outgoing tube.

Z = Desired minimum taper of the mandrel.

L_i= Clearance between inside diameter of ingoing tube and mandrel.

L_a = Clearance between outside diameter of ingoing tube and mandrel.

x/L= Point 'x' of the working zone of the groove related to the working section length 'L'.

n_x = Correction factor for clearance to be allowed for between ingoing tube and mandrel and between outgoing tube and groove diameter.

$$= \frac{(\frac{x}{L} - 0.7)^2}{(1-0.7)^2}, \frac{x}{L} > 0.7$$

$$= 0 \quad , \frac{x}{L} < 0.7$$

a) Design with cone as basis :

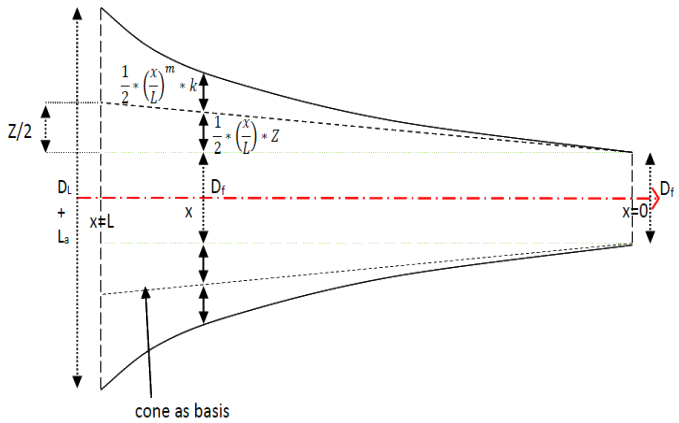

Fig [3] : Profile of groove root diameter.

Diameter of groove at x is given by:

$$D_x = D_f + k * \left(\frac{x}{L}\right)^m + \left(\frac{x}{L}\right) * Z + n_x * (L_i + L_a)$$

Boundary Conditions:

$$at\ x = L,\ \ D_x = D_L + L_a\ ,$$

So we get:

$$D_L + L_a = D_f + k + Z + L_i + L_a$$

Thus,

$$k = D_L - D_f - L_i - Z$$

$$\boldsymbol{D_x = D_f + \left(\frac{x}{L}\right)^m * (D_L - D_f - L_i - Z) + n_x * (L_i + L_a)}$$

2) Derivation Of Mandrel Profile:

$$\boldsymbol{d_x = d_f + C_x(d_l - d_f - L_i) + \left(\frac{x}{L}\right) * Z}$$

Where, d_x = Mandrel diameter at point 'x' of the working section of the mandrel.
C_x= Factor for the shape of the groove and mandrel curve.
d_l= Inside diameter of the ingoing tube.
d_f= Inside diameter of the outgoing tube.
Z = Desired minimum taper of the mandrel.
L_i= Clearance between inside diameter of ingoing tube and mandrel.
L_a = Clearance between outside diameter of ingoing tube and mandrel.
x/L = Point 'x' of the working zone of the mandrel related to the working section length 'L'.

a) Desing with Cylinder as Basis:

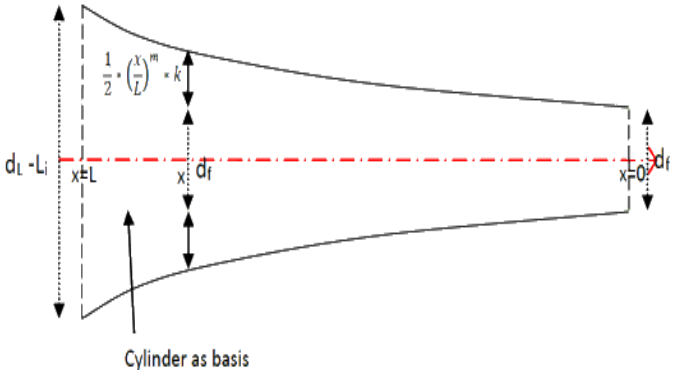

Diameter of mandrel at x is given by:

$$d_x = d_f + k * \left(\frac{x}{L}\right)^m$$

Boundary Condition:

$$at\ x = L, d_x = d_L - L_i\ ,$$

So we get,

$$d_L - L_i = d_f + k$$

Thus,

$$k = d_L - d_f - L_i$$

$$\boldsymbol{d_x = d_f + \left(\frac{x}{L}\right)^m (d_l - d_f - L_i)}$$

b) Design with cone as basis (with minimum taper):

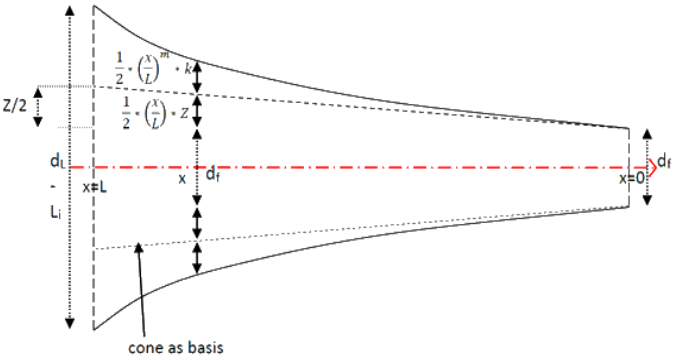

Diameter of mandrel at x is given by:

$$d_x = d_f + k * \left(\frac{x}{L}\right)^m + \left(\frac{x}{L}\right) * Z$$

Boundary Conditions:

$$at\ x = L,\quad d_x = d_L - L_i\ ,$$

So we get,

$$d_L - L_i = d_f + k + Z$$

Thus,

$$k = d_L - d_f - L_i - Z$$

$$\boldsymbol{d_x = d_f + \left(\frac{x}{L}\right)^m (d_l - d_f - L_i - Z) + \left(\frac{x}{L}\right) * Z}$$

D. Calculation of Side Relief

Side relief is necessary because the tube diameter is greater than the groove root circle diameter, which has to be

accommodated the tube diameter. Therefore, the width of the groove must always be great enough so that the pass can just accommodate the tube without nipping it. It is necessary to calculate which tube diameter is to be correlated to which position of the groove, the influencing factors being the feed increment, and the diameter and sectional area reduction patterns.

For all the divisional points the product of feed and partial elongation is determined by equation:

$$VS = \Delta x_i = f * \frac{A_o}{A_i}$$

Where,

$\boldsymbol{A_o}$ =cross-sectional area of a hollow

$\boldsymbol{A_i}$ = cross-sectional area of a deformed tube element at the i[th] shot.

Now a graph is plotted with the co-ordinates (x_i+VS , $D_x/2$) as shown :

The side relief at I[th] point is given by:

$$F_x = D_{x_{i-1}} - D_{x_i}$$

SELECTION OF PITCH-PINION ROLLS

Both 75VMR and 150 VMR have different pinions having separate pitch diameters. The selection is based on following equation.

$$D_W - D_R = \left(\frac{D_L + D_f}{2}\right) * SF$$

Where

D_W = diameter of the die.

D_R= diameter of pitch pinion.

D_l = Outside diameter of the ingoing tube.

D_f= Outside diameter of the outgoing tube.

SF= slip factor

There are three pinion diameters available for 75 VMR pilger mill. The table below lists the available pinion sizes and roll diameter.

D_W	370mm
D_{R1}	348mm
D_{R2}	336mm
D_{R3}	324mm

Circumferential speed of the pitch pinion should be same as the longitudinal speed of the roll, when they are ideally matched.

When the calculated value using the above formula for a particular tube is in between the standard pitch pinion diameter, it is better to take lower pinion diameter than the bigger one.

If the pitch pinion diameter is larger than the required one, the tube moves forward without feed. This is because the velocity of the die groove is slower than the velocity of the pinion. So we should always try to match the die dia. and pinion dia. to the extent possible.

If the pinion diameter selected is smaller than the required one, the loading on the tube feeding device will be more due to increased back forces.

7. STRAIN CALCULATION IN EACH SECTION

Considering section 1

$\partial\varepsilon_l = \ln\left(\frac{A_i}{A_{i-1}}\right)$, $\partial\varepsilon_r = \ln\left(\frac{tm_{1i}}{tm_{3i-1}}\right)$& $\partial\varepsilon_\theta = -(\partial\varepsilon_l + \partial\varepsilon_r)$

Where,

$\partial\varepsilon_l$ = Axial strain in section 1 at i[th]shot.

$\partial\varepsilon_r$ = Radial strain in section 1 at i[th]shot.

$\partial\varepsilon_\theta$ =Circumferential strain in section 1 at i[th] shot.

A_i =Area of the cross-section at i[th]shot.

A_{i-1} =Area of the cross-section at i-1[th] shot.

tm_{1_i} =Mean thickness of the section 1 at i[th]shot.

$tm_{3_{i-1}}$ =Mean thickness of the section 3 at i-1[th] shot.

Considering section 2

$\partial\varepsilon_l = \ln\left(\frac{A_i}{A_{i-1}}\right)$, $\partial\varepsilon_r = \ln\left(\frac{tm_{2i}}{tm_{1i-1}}\right)$& $\partial\varepsilon_\theta = -(\partial\varepsilon_l + \partial\varepsilon_r)$

Where,

$\partial\varepsilon_l$ = Axial strain in section 2 at i[th]shot.

$\partial\varepsilon_r$ = Radial strain in section 2 at i[th]shot.

$\partial\varepsilon_\theta$ =Circumferential strain in section 2 at i[th] shot.

A_i =Area of the cross-section at i[th]shot.

A_{i-1} =Area of the cross-section at i-1[th] shot.

tm_{2_i} =Mean thickness of the section 2 at i[th]shot.

$tm_{1_{i-1}}$ =Mean thickness of the section 1 at i-1[th] shot.

Considering section 3

$\partial\varepsilon_l = \ln\left(\frac{A_i}{A_{i-1}}\right)$, $\partial\varepsilon_r = \ln\left(\frac{tm_{3i}}{tm_{2i-1}}\right)$& $\partial\varepsilon_\theta = -(\partial\varepsilon_l + \partial\varepsilon_r)$

Where,

$\partial\varepsilon_l$ = Axial strain in section 3at i[th]shot.

$\partial\varepsilon_r$ = Radial strain in section 3 at i[th]shot.

$\partial\varepsilon_\theta$ =Circumferential strain in section 3 at i[th] shot.

A_i =Area of the cross-section at i[th]shot.

A_{i-1} =Area of the cross-section at i-1[th] shot.

tm_{3_i} =Mean thickness of the section 3 at i[th]shot.

$tm_{2_{i-1}}$ =Mean thickness of the section 2 at i-1[th] shot.

STRESS-STRAINS RELATIONSHIPS

The following are the equations of plasticity which have been considered in each section to relate all stress and strains

8.1 Hencky equation

Derivation: TheLevi Mises equations are:

$\partial\varepsilon_1 = \frac{2\partial\lambda}{3}\left\{\sigma_1 - \left(\frac{\sigma_2+\sigma_3}{2}\right)\right\}$,$\partial\varepsilon_2 = \frac{2\partial\lambda}{3}\left\{\sigma_2 - \left(\frac{\sigma_3+\sigma_1}{2}\right)\right\}$&$\partial\varepsilon_3 = \frac{2\partial\lambda}{3}\left\{\sigma_3 - \left(\frac{\sigma_1+\sigma_2}{2}\right)\right\}$

Thus,

$\partial\varepsilon_1 - \partial\varepsilon_2 = (\sigma_1 - \sigma_2) * \partial\lambda$,$\partial\varepsilon_2 - \partial\varepsilon_3 = (\sigma_2 - \sigma_3) * \partial\lambda$**&**$\partial\varepsilon_3 - \partial\varepsilon_1 = (\sigma_3 - \sigma_1) * \partial\lambda$

From Von-Mises yield criteria, we have:

$\bar{\sigma} = \frac{1}{\sqrt{2}} * \{(\sigma_1 - \sigma_2)^2 + (\sigma_2 - \sigma_3)^2 + (\sigma_3 - \sigma_1)^2\}^{0.5}$, and

$$\overline{\partial\varepsilon} = \frac{\sqrt{2}}{3} * \{(\partial\varepsilon_1 - \partial\varepsilon_2)^2 + (\partial\varepsilon_2 - \partial\varepsilon_3)^2 + (\partial\varepsilon_3 - \partial\varepsilon_1)^2\}^{0.5}$$

By combining levi-mises and von-mises we get:

$$\partial\lambda = \frac{3\overline{\partial\varepsilon}}{2\bar{\sigma}}$$

Thus,

$\frac{\partial\varepsilon_1 - \partial\varepsilon_2}{\sigma_1 - \sigma_2} = \frac{3\overline{\partial\varepsilon}}{2\bar{\sigma}}$, $\frac{\partial\varepsilon_2 - \partial\varepsilon_3}{\sigma_2 - \sigma_3} = \frac{3\overline{\partial\varepsilon}}{2\bar{\sigma}}$**&**$\frac{\partial\varepsilon_3 - \partial\varepsilon_1}{\sigma_3 - \sigma_1} = \frac{3\overline{\partial\varepsilon}}{2\bar{\sigma}}$

Finally we get.

$$\frac{\sigma_\theta - \sigma_l}{\partial\varepsilon_\theta - \partial\varepsilon_l} = \frac{\sigma_l - \sigma_r}{\partial\varepsilon_l - \partial\varepsilon_r} = \frac{\sigma_r - \sigma_\theta}{\partial\varepsilon_r - \partial\varepsilon_\theta} = \frac{2\bar{\sigma}}{3\overline{\partial\varepsilon}} = k$$

Thus,

$\sigma_\theta - \sigma_l = \left(\frac{2\bar{\sigma}}{3\overline{\partial\varepsilon}}\right) * (\partial\varepsilon_\theta - \partial\varepsilon_l)$ ---------- (i)

$\sigma_l - \sigma_r = \left(\frac{2\bar{\sigma}}{3\overline{\partial\varepsilon}}\right) * (\partial\varepsilon_l - \partial\varepsilon_r)$ ---------- (ii)

$\sigma_r - \sigma_\theta = \left(\frac{2\bar{\sigma}}{3\overline{\partial\varepsilon}}\right) * (\partial\varepsilon_r - \partial\varepsilon_\theta)$ ---------- (iii)

8.2 Equilibrium Equation In Radial Direction

The normal radial stress at a radius r is σ_r and at a radius r + dr , is $\sigma_r + \frac{d\sigma_r}{dr}dr$

The equation of equilibrium for the element as shown is :

$$r\sigma_r d\theta + \sigma_\theta dr d\theta - \left(\sigma_r + \frac{d\sigma_r}{dr}dr\right)(r + dr)d\theta = 0$$

$$\sigma_\theta - \sigma_r = r\frac{d\sigma_r}{dr}$$

$$\sigma_{rb} - \sigma_{ra} = \int_{ra}^{rb} (\sigma_r - \sigma_\theta)\frac{\partial r}{r}$$

Where,

σ_{rb} = Radial Stress at the outside of the tube

σ_{ra}= Radial Stress at the inside of the tube

ra = Inside radius of the tube

rb = Outside radius of the tube

Substituting eq. (iii), we get:

$$\sigma_{rb} - \sigma_{ra} = \int_{ra}^{rb} \left(\frac{2\bar{\sigma}}{3\overline{\partial\varepsilon}}\right) * (\partial - \partial\varepsilon_\theta)\frac{\partial r}{r}$$

30

Thus,

$\boldsymbol{\sigma_{rb} - \sigma_{ra} = \left(\frac{2\bar{\sigma}}{3\overline{\partial\varepsilon}}\right) * (\partial\varepsilon_r - \partial\varepsilon_\theta) * \ln\frac{rb}{ra}}$---------- (iv)

And, the approximate equation for mean radial stress is given by:

$\boldsymbol{\sigma_r = (\frac{\sigma_{rb} + \sigma_{ra}}{2})}$ ---------- (v)

Considering flange part(Section 3)

The boundary condition at the inside surface of the flange part is:

$\sigma_{r\sigma a_{ra3}} = 0$,

Thus

$\sigma_{r\sigma b_{rb3}} = \left(\frac{2\bar{\sigma}\bar{\sigma}}{3\partial\epsilon\overline{\partial\varepsilon}}\right) * (\partial\varepsilon_r\partial\varepsilon_\theta\partial\varepsilon_r - \partial\varepsilon_\theta) * \ln\frac{rb}{ra}\frac{rb}{ra}$ -------- -- (from eq. (iV))

$\sigma_{r3} = \frac{\sigma_{rb3}}{2}$ -------- -- (from eq. (v))

$\sigma_{\theta 3} = \sigma_{r3} + \left(\frac{2\bar{\sigma}}{3\overline{\partial\varepsilon}}\right) * (\partial\varepsilon_\theta - \partial\varepsilon_{r3})$ -------- -- (from eq. (iii))

$\sigma_{l3} = \sigma_{r3} + \left(\frac{2\bar{\sigma}}{3\overline{\partial\varepsilon}}\right) * (\partial\varepsilon_{l3} - \partial\varepsilon_{r3})$ ---------- (from eq. (ii))

Considering groove part (section 1**)**

For equilibrium of force in the circumferential direction (refer to figure) :

$$\sigma_{\theta_1} * t_{m_1} = \sigma_{\theta_3} * t_{m_3}$$

Thus

$\sigma_{r_1} = \sigma_{\theta_1} - \left(\frac{2\bar{\sigma}}{3\overline{\partial\varepsilon}}\right) * (\partial\varepsilon_{r_1} - \partial\varepsilon_{\theta_1})$ -------- -- (from eq. (iii))

$\sigma_{l_1} = \sigma_{r_1} + \left(\frac{2\bar{\sigma}}{3\overline{\partial\varepsilon}}\right) * (\partial\varepsilon_{l_1} - \partial\varepsilon_{r_1})$ --------- (from eq. (ii))

$\sigma_{rb_1} = \sigma_{r_1} + \frac{\left(\frac{2\bar{\sigma}}{3\overline{\partial\varepsilon}}\right) * (\partial\varepsilon_{r_1} - \partial\varepsilon_{\theta_1}) * \ln\frac{rb}{ra}}{2}$ ---------- (from eq. (iv) & (v))

$\sigma_{ra_1} = \sigma_{r_1} - \frac{\left(\frac{2\bar{\sigma}}{3\overline{\partial\varepsilon}}\right) * (\partial\varepsilon_{r_1} - \partial\varepsilon_{\theta_1}) * \ln\frac{rb}{ra}}{2}$ ---------- (from eq. (iv) &

(v)Considering groove part (section 2)

For equilibrium of force in the circumferential direction (refer to above figure) :

$\sigma_{\theta_2} * t_{m_2} = \sigma_{\theta_3} * t_{m_3}$

Thus

$\sigma_{r_2} = \sigma_{\theta_2} + \left(\frac{2\bar{\sigma}}{3\overline{\partial\varepsilon}}\right) * (\partial\varepsilon_{r_2} - \partial\varepsilon_{\theta_2})$---------- (from eq. (iii))

$\sigma_{l_2} = \sigma_{r_2} + \left(\frac{2\bar{\sigma}}{3\overline{\partial\varepsilon}}\right) * (\partial\varepsilon_{l_2} - \partial\varepsilon_{r_2})$ ---------- (from eq. (ii))

$\sigma_{rb_2} = \sigma_{r_2} + \frac{\left(\frac{2\bar{\sigma}}{3\overline{\partial\varepsilon}}\right) * (\partial\varepsilon_{r_2} - \partial\varepsilon_2) * \ln\frac{rb}{ra}}{2}$ ---------- (from eq. (iv) & (v))

$\sigma_{ra_2} = \sigma_{r_2} - \frac{\left(\frac{2\bar{\sigma}}{3\overline{\partial\varepsilon}}\right) * (\partial\varepsilon_{r_2} - \partial\varepsilon_2) * \ln\frac{rb}{ra}}{2}$ ---------- (from eq. (iv) & (v))

Contact Length

Neumann and Siebel distinguished two parts in contact length:

i. In L_{d1}, the tube is in contact with both mandrel and die. As this part is in contact with both die and mandrel hence it's length is proportional to the difference between the slopes of the two.
ii. In L_{d2}, the contact is lost with mandrel as a wave of material is pushed forward by the moving die.. As this part has lost contact with mandrel so its length will be proportional to the slope of mandrel.

Hence by rolling analogy, the final equation is:

$$L_d = \sqrt{2R_x.f.\frac{A_o}{A_i}}.\left(\sqrt{\varphi(x)-\delta(x)}+\sqrt{\delta(x)}\right)$$

Where,
Rx = Die radius at point x
f = feed
A_o,A_i, = Initial and intermediate(at position x) cross-sectional area of the tube$\varphi(x),\delta(x)$ = Die and mandrel conicity

8.3 FUNDAMENTAL EQUATION FOR ROLL SEPARATING FORCE

The Roll separating force P is determined as a summation of the product of outside radial stress $\sigma_{rbj}$and the projected contact area (S_j) for each section of the cross-section of the tube.
$S_j = L_d$ * projected outer width of each section.
$P = \sum$

FORCE ON MANDREL

The Mandrel force F is determined as a summation of the product of inner radial stress $\sigma_{raj}$and the projected contact area (S_j) for each section of the cross-section of the tube.
$S_j = L_{d1}$ * projected inner width of each section.
$P = \sum$

AXIAL FORCE

Axial force is determined by summation of the product of stress $\sigma_{l_j}$and cross-section area A_j of the tube.

$F= \sum$

MANDREL STRESS

The crushing stress on the mandrel is given by dividing the force on the mandrel with the projected area of contact (S_j) for each section of the cross-section of the tube on the mandrel.
$S_j = L_{d1}$ * projected inner width of each section.

IV. CONCLUSION

Various hypotheses, theories and assumptions and essential relations used in the analysis of plastic deformation are derived from the principles of Theory of Plasticity which are incorporated in this paper. The experimental determination of the three dimensional displacement and strain fields during the cold pilger rolling is very extremely demanding task. In practice, due to large rolling velocities it is limited only to one deformation cycle. Eventually FDM method is applied to determine locations of the marking grid after deformation. Due to high deformation and friction of the pilger rolling the grids were disappearing and accurate dislodging estimation became difficult. Here, a graph is generated by the equivalent strain calculated using FDM methods by comparing initial and final coordinates of grid nodes. The issue of node dispersion at the internal surface of the tube and along the cone surfaces was not unraveled as in genuine mechanical methodology it is extremely difficult to make the estimations for a solitary deformation cycle that last 0.4 seconds due to high rolling speed. However, at this stage due to large and substantial calculation errors these results can't be utilized as valuable data during the process of say, tool design. Additionally, obtained results are only for the outer surface of the tube. The resulted strain field can't be considered as three dimensional, in light of the fact that the internal surface is disregarded during calculations

Acknowledgment

We very thankful to all our friends those who have helped us directly or indirectly for accomplishment of this work, any anonymous reviewers for their detailed comments that improved this paper, all Resources and Managements for Invitation and Publications.

References

[1] "Mechanical Metallurgy" by George E. Dieter

[2] M. Furugen and C. Hayashi, "Application of Theory of Plasticity to the cold Pilgering of tubes", J. Mech. Work. Technol., (1984) 273-286.

[3] "A New Fabrication Process for Zr-Lined Zircalloy-2 Tubing" by Hideaki Abe , Kiyoko Taketa, Akihiro Uehira, Hiroyuki Anada and Munekatsu Furugen.

[4] "Material Deformation During The cold Tube Rolling Process Realized on Generation of Pilger Mills" by J.Osika, H.Palkowski, K.Swiatkowski, D.Pociecha, A.Kula.

Web References :

[5] www.nfc.gov.in

[6] www.sciencedirect.com

[7] www.springer.com